Chapter 25

A new limit of the $\mu^+ \to e^+\gamma$ decay from the MEG experiment

Angela Papa

Abstract

A search for the decay $\mu^+ \to e^+\gamma$ is going on at PSI. The 2009 collected data from the initial three months of operation of the MEG experiment yields an upper limit BR($\mu^+ \to e^+\gamma$) $\leq 2.8 \times 10^{-11}$ (90% C.L.). The analysis of the combined 2009 and 2010 data sample gives a 90% C.L. upper limit of 2.4×10^{-12}, constituting the most stringent limit on the existence of this decay to date.

25.1. Introduction

Lepton flavour violation (LFV) research is presently one of the most exciting branches of particle physics. Flavour violating processes, such as $\mu^+ \to e^+\gamma$, which are not predicted by the Minimal Standard Model (SM), are very sensitive to the physics beyond it. Neutrino oscillations are now an established fact, which can be accomodated in the SM by including right-handed massive neutrinos and mixing. This modified SM predicts unmeasureable branching ratios (BR) for lepton violating decays. Supersymmetric GUT theories naturally house finite neutrino masses and predict rather large and measurable branching ratios for LFV decays. The $\mu^+ \to e^+\gamma$ process is therefore a powerful tool to investigate physics beyond the SM, since: a) the present experimental upper limit is $\mathrm{BR} = 1.2 \cdot 10^{-11}$ at 90% C.L. (by the MEGA collaboration [1]) and b) supersymmetric GUT models, such as SO(10) SUSY-GUT or SU(5) SUSY-GUT, predict $\mathrm{BR} \approx 10^{-14} - 10^{-11}$ [2,3,4,5,6].

The aim of the MEG experiment is to measure the branching ratio of the rare muon decay $\mathrm{BR} = \frac{\mu^+ \to \mathrm{e}^+\gamma}{\mu^+ \to \mathrm{e}^+\nu_\mathrm{e}\overline{\nu}_\mu}$ at a sensitivity of $\approx 10^{-13}$, two orders of magnitude better than the present experimental limit and within the region of theoretical predictions [7].

To reach this goal, the experiment must use the most intense continuous muon beam available ($\approx 10^8 \mu/\mathrm{s}$) and obtain the highest energy, time and space resolutions, today reachable. MEG started to collect data at

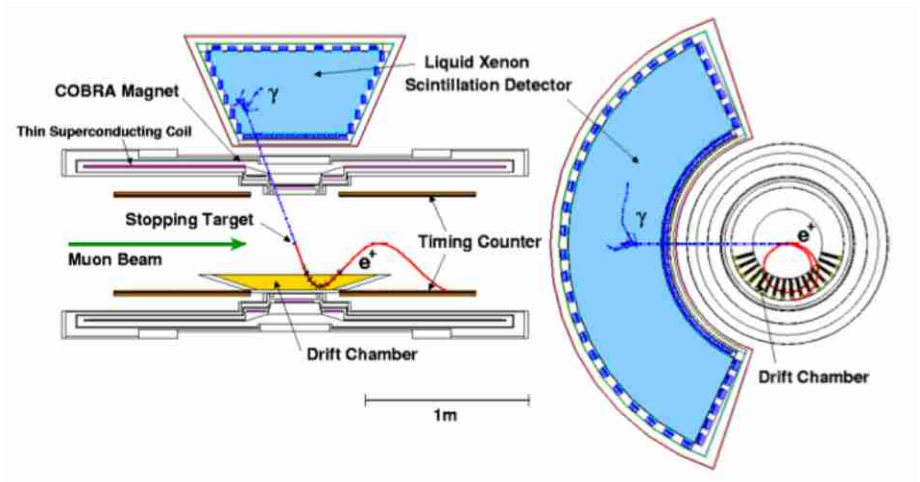

Figure 25.1. The MEG experiment layout.

the end of 2008. During 2009 a large part of the data taking time was devoted to calibration measurements and detector performance optimizations; a new physics data sample was collected at the end of this year in 1.5 months of acquisition time. We have continued to take data during 2010 and the final analysis of this sample is going on. Our final result will include both 2009 and 2010 data samples. A description of the main features of each subdetector and of the measured resolutions are given and the preliminary results of the search for $\mu^+ \to e^+\gamma$ decay based on the 2009 data sample are presented.

The event signature of the $\mu^+ \to e^+\gamma$ decay at rest is a positron and a photon in timing coincidence, moving collinearly back-to-back with their energies equal to half the muon mass ($m_\mu/2 = 52.8$ MeV). Positive muons are used because they can be stopped in a target without being captured by a nucleus.

Two kinds of background are present: a) the prompt background from the radiative muon decay, $\mu^+ \to e^+\nu_e\overline{\nu}_\mu\gamma$ and b) the uncorrelated background due to an accidental coincidence between a positron from the normal muon decay $\mu^+ \to e^+\nu_e\overline{\nu}_\mu$ and a high energy photon from radiative muon decay or positron annihilation in flight. The latter is the main background source and we evaluated its effective branching ratio at level of $\leq 10^{-13}$.

$\approx 10^{14}$ muons were stopped in the target. A data reduction was performed and the pre-selected events were further processed. The events falling into a pre-defined window in the E_γ vs $t_{e\gamma}$ plane ("blinding-box"), which includes the signal region, were saved in separate hidden files; the $\mu \to e\gamma$ decay was searched within this sample. The other events ("side-bands") were used for optimizing the analysis parameters and for studying the background.
A likelihood analysis was performed to determine the B.R. upper limit on $\mu \to e\gamma$ decay.

25.2. Experimental set-up

A schematic layout of the MEG detector is shown in the Fig. 25.1.
Abundant low energy muons can be produced at high intensity proton accelerators. The so-called surface

muons are obtained by bombarding protons in a thick production target and come out from the two-body decays of positive pions that stop near the surface of the target, with a sharp momentum of approximately 29 MeV/c. Because of their low momentum and narrow momentum spread (typically 8% FWHM), a thin target ($\approx 10mg \cdot cm^{-2}$) can be employed, with several advantages: good identification of decay region (thanks also to the small beam spot size $\sigma_x = \sigma_y \approx 10mm$), low positron momentum degradation, minimum positron annihilation (a source of γ background). The dc beam structure is also extremely important because the accidental background increases quadratically with the beam rate and this feature gives a lowest instantaneous background compared to a pulsed beam.

The positron momentum, direction and time are measured by means of a novel spectrometer made by an array of 16 modules of low-mass drift chambers, inserted in a superconducting magnet, wich supplies a gradient field along the beam direction (Z-coordinate) with a maximum intensity at the center of 1.25 Tesla. The non-uniformity of B-field produces a constant projected radius of the positron trajectory, indipendently of the emitted positron angle and function only of the positron energy. Moreover low momentum positrons are swept away, without hitting the chambers, avoiding to busy the detector and to have not useful hits in the recostruction.

Two sectors of 15 scintillating bars, mounted at each end of the spectometer and equipped with PMTs working in a high magnetic field region, provides the best timing measurement at this energy.

An innovative homogeneous liquid xenon calorimeter performes a precise measurement of the convertion point, timing and energy of the γ ray. 846 photomultipliers are fully immersed in the xenon and only the VUV scintillating light is collect to preserve the rapity of detector based on the short scintillation time constants (22 and 45 ns).

The stability of the all detectors is continuously monitored and the performances are measured by means of complementary calibration methods. The position, energy and timing resolutions of the calorimeter at an energy closer to the signal one are determined selecting 55 MeV γ ray from the π^0 decay, produced from the pion charge exchange reaction $\pi^- p \to \pi^0 n$ at rest. Energy calibration and linearity, stability, uniformity and purity are frequently measured illuminating the inner face of the calorimeter with a sharp gamma line at 17.6 MeV from the resonant reaction $Li(p,\gamma)Be$. The optical properties of the Xenon and the PMT's parameters (gain and QE) are extracted using Point-like Am-α source and LED. A 9 MeV line from the capture in nickel of neutrons from a pulsed and triggerable deuteron-deuteron neutron generator allows one to check the stability of the LXe detector even during data taking. The relative time between the TC and LXe detector is monitored using radiative muon decay events and 2 coincident γ from the $B(p,2\gamma)C$ reaction. The absolute scale of the spectrometer is fixed by the Michel energy spectrum edge and a new method based on monochromatic Mott scattered positrons has being optimized to be used as standard tool for a deeper understanding of the spectrometer.

An efficienty and flexible trigger which use only the fast detectors was developed to select with high efficiency the signal and to accomodate the different calibration methods. The DAQ is designed to digitize all waveforms, with an excellent capability to reject the pile-up. It is based on the multi-GHz domino ring sampler chip (DRS), which can sample ten analogue input channels into 1024 sampling cells each at speeds of up to 4.5 GHz. The sampling speed for the drift chamber anode and cathode signals is 500 MHz, while that of the PMT signals from the photon detector and timing counters is 1.6 GHz.

A detailed GEANT 3.21 based Monte Carlo simulation of the full apparatus (transport system and detector) was developed and used throughout the experiment, from the design and optimization of all sub-systems to the calculation of acceptances and efficiencies.

25.3. Resuls from 2009 data sample

The data sample analyzed here was collected between September and December 2008 and corresponds to $\approx 9.5 \times 10^{13}$ muons stopping in the target. The collected sample is saved and a preliminary data reduction

is performed. These pre-selected events are further processed. The events falling into a pre-defined window ("blinding-box"), containing the signal region on the E_γ-ray and on the $t_{e\gamma}$, were saved in separate hidden files; the $\mu \to e\gamma$ decay is searched within this sample. The other events ("side-bands") are used for optimizing the analysis parameters and for studying the background. The blinding-box is opened after completing the optimization of the analysis algorithms and the background studies.

A candidate $\mu \to e\gamma$ event is characterized by the measurement of five kinematical parameters: positron energy E_e, gamma energy E_γ, relative time between positron and gamma $t_{e\gamma}$ and the opening angles between the two particles $\theta_{e\gamma}$ and $\phi_{e\gamma}$.

A likelihood function is built in terms of the signal and the two kinds of background: the radiative Michel decay and the accidental background. A probability density function (PDF), depending on the five kinematical parameters, is associated to each component; the likelihood has the following expression:

$$\mathcal{L}(N_{sig}, N_{RMD}, N_{BG}) = \frac{N^{N_{obs}} e^{-N}}{N_{obs}!} \prod_{i=1}^{N_{obs}} \left[\frac{N_{sig}}{N} S + \frac{N_{RMD}}{N} R + \frac{N_{BG}}{N} B \right]. \tag{25.1}$$

The signal PDF S is obtained as the product of the PDFs for the five observables (E_γ, E_e, $t_{e\gamma}$, $\theta_{e\gamma}$ and $\phi_{e\gamma}$). The radiative Michel decay PDF R is the product of the theoretical PDF (in terms of the correlated E_γ, E_e, $\theta_{e\gamma}$ and $\phi_{e\gamma}$), folded with the detector response, and the measured $t_{e\gamma}$ PDF (the same of the signal one); the PDF B is the product of the background spectra for the five observables, which are precisely measured in the data sample in the side-bands.

The event distributions of the five observables for all events in the analysis window are shown in Fig. 25.2, togheter with the projections of the fitted likelihood function. The 90% confidence intervals on N_{sig} and N_{RMD} are determined by the Feldman-Cousins approach [8]. A contuour of 90% C.L. on the (N_{sig}, N_{RMD})-plane is constructed by means of a toy Monte Carlo simulation. On each point on the contour, 90% of the simulated experiments give a likelihood ratio ($\mathcal{L}/\mathcal{L}_{max}$) larger than that of the ratio calculated for the data. The limit for N_{sig} is obtained from the projection of the contour on the N_{sig}-axis. The obtained upper limit at 90% C.L. is $N_{sig} < 14.7$, where the systematic error is included. The largest contributions to the systematic error are from the uncertainty of the selection of photon pile-up events, the photon energy scale, the response function of the positron energy and the positron angular resolution.

The upper limit on BR($\mu^+ \to e^+\gamma$) was calculated by the C.L. intervals normalizing the upper limit on N_{sig} to the Michel positrons counted simultaneously with the signal, with the same analysis cuts, assuming BR($\mu^+ \to e^+\nu_e\overline{\nu}_\mu$) ≈ 1. This method has the advantage of being indipendent of the instantaneous beam rate and is nearly insensitive to the positron acceptance and efficiency factors associated with the DCH and TC, which differ only for small momentum dependent effects between the signal and the normalization sample.

The branching ratio can be written as:

$$\mathrm{BR}(\mu^+ \to \mathrm{e}^+\gamma) = \frac{\mathrm{N_{sig}}}{\mathrm{N_{e\nu\overline{\nu}}}} \times \frac{\mathrm{f^E_{e\nu\overline{\nu}}}}{\mathrm{P}} \times \frac{\epsilon^{\mathrm{trg}}_{\mathrm{e\nu\overline{\nu}}}}{\epsilon^{\mathrm{trg}}_{\mathrm{e\gamma}}} \times \frac{\mathrm{A^{TC}_{e\nu\overline{\nu}}}}{\mathrm{A^{TC}_{e\gamma}}} \times \frac{\epsilon^{\mathrm{DCH}}_{\mathrm{e\nu\overline{\nu}}}}{\epsilon^{\mathrm{DCH}}_{\mathrm{e\gamma}}} \times \frac{1}{\mathrm{A^g_{e\gamma}}} \times \frac{1}{\epsilon_{\mathrm{e\gamma}}} \tag{25.2}$$

where $N_{e\nu\overline{\nu}}$ is the number of detected Michel positrons with $50 \leq E_e \leq 56$ MeV; P is the prescale factor in the trigger used to select Michel positrons; $f^E_{e\nu\overline{\nu}}$ is the fraction of Michel positron spectrum above 50 MeV; $\epsilon^{trg}_{e\gamma}/\epsilon^{trg}_{e\nu\overline{\nu}}$ is the ratio of signal-to-Michel trigger efficiencies; $A^{TC}_{e\gamma}/A^{TC}_{e\nu\overline{\nu}}$ is the ratio of the signal-to-Michel DCH-TC matching efficiency; $\epsilon^{DCH}_{e\gamma}/\epsilon^{DCH}_{e\nu\overline{\nu}}$ is the ratio signal-to-Michel DCH recostruction efficiency and acceptance; $A^g_{e\gamma}$ is the geometrical acceptance for gamma signal given an accepted signal positron; $\epsilon_{e\gamma}$ is the efficiency of gamma recostruction and selection criteria.

The quoted limit on the branching ratio of the $\mu^+ \to e^+\gamma$ decay is therefore:

$$\mathrm{BR}(\mu^+ \to \mathrm{e}^+\gamma) \leq 2.8 \times 10^{-11}\ (90\%\mathrm{C.L.}) \tag{25.3}$$

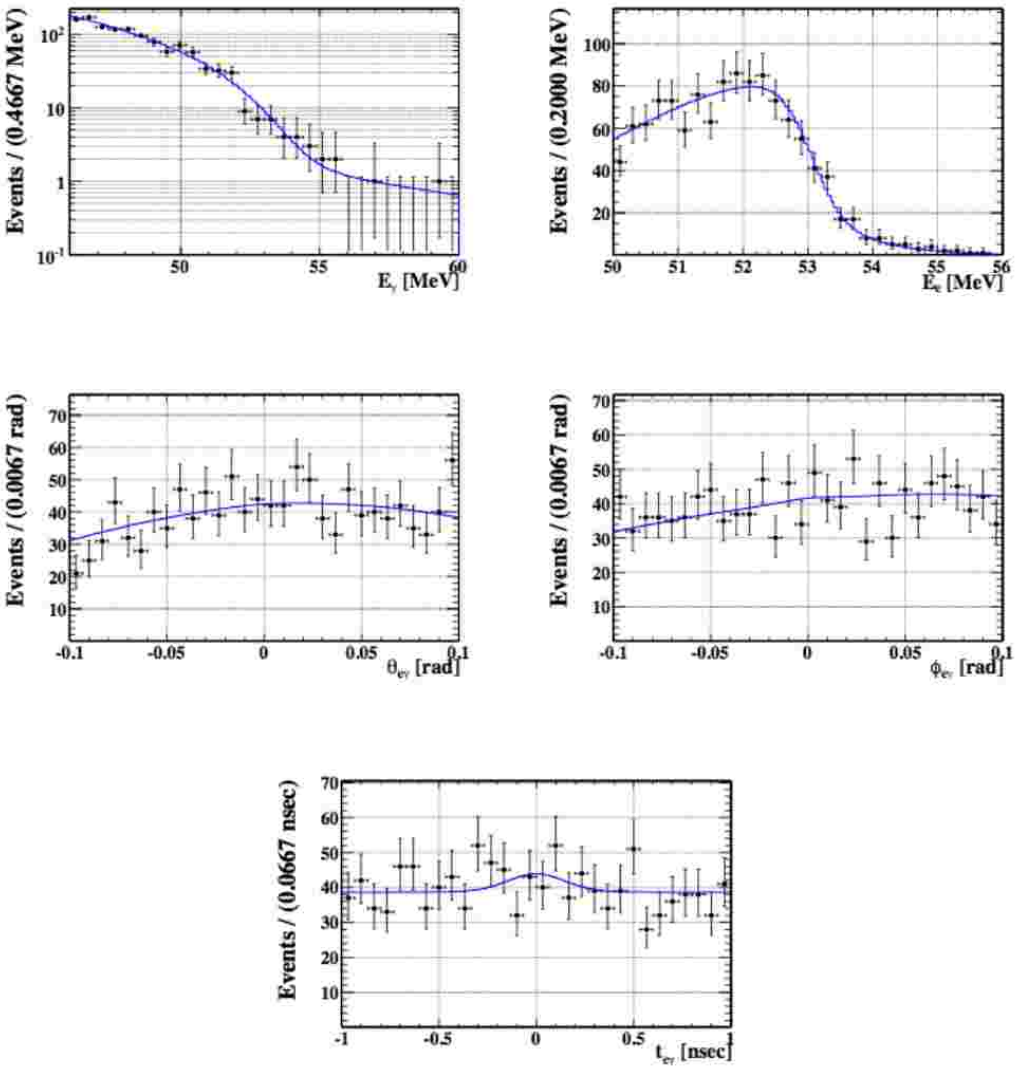

Figure 25.2. The event distributions of the five observables for all events in the analysis window. The blu line shows the projections of the fitted likelihood function.

where the systemetic uncertainty on the normalization is taken into account [9].

The analysis of the 2010 data is now finished and the results of both 2009 and 2010 data are available. The likelihood analysis of the combined data sample, which corresponds to a total of 1.8×10^{14} muon decays, gives an upper limit of:

$$\mathrm{BR}(\mu^+ \to \mathrm{e}^+\gamma) \leq 2.4 \times 10^{-12} \ (90\%\mathrm{C.L.}) \tag{25.4}$$

This is the most stringent limit on the existence of this decay to date [10].

REFERENCES

1. M.L. Brooks et al. (MEGA collaboration) *Phys. Rev. Lett.*, Vol. 83, 1521 (1999).
2. R. Barbieri and L.J. Hall *Phys. Lett. B*, Vol. 338, 212 (1994).
3. R. Barbieri, L.J. Hall and A. Strumia *Nucl. Phys. B*, Vol. 445, 219 (1995).
4. Y. Kuno and Y. Okada *Rev. Mod. Phys.*, Vol. 73, 151 (2001).
5. M. Raidal et al. *arXiv:0801.1826v1*, "Flavour physics of leptons and dipole moments".
6. L. Calibbi et al. *hep-ph/0605139*, "Lepton flavour violation from SUSY-GUTs: where do we stand for MEG,PRISM/PRIME and a super flavour factory".
7. A.Baldini et al. *Research Proposal to INFN* (2002).
8. G. J. Feldman and R. D. Cousins *Phys. Rev.*, Vol. D57, 3873 (1998).
9. J. Adam et al (MEG Collaboration) *Nucl. Phys. B*, Vol. 834, 1 (2010).
10. J. Adam et al (MEG Collaboration) *Phy. Rev. Lett.*, Vol. 107, 171801 (2011).